A borehole video examination of debris within the terminus of a polythermal glacier, Storglaciären, northern Sweden.

Matthew Dettinger
Senior Integrative Exercise
March 10, 2008

Submitted in partial fulfillment of the requirements for a Bachelor of Arts degree from Carleton College, Northfield, Minnesota

TABLE OF CONTENTS

A borehole video examination of debris within the terminus of a polythermal glacier, Storglaciären, northern Sweden.

Matthew Dettinger
Carleton College
Senior Integrative Exercise
March 10, 2008

Advisors:
Sarah Titus, Carleton College
Pete Moore, Iowa State University

ABSTRACT

Storglaciären is a well-studied polythermal glacier in the Swedish Arctic. The majority of Storglaciären slides over the bed, but the glacier becomes frozen to the bed at the basal thermal transition (BTT) near the terminus. Downglacier of the transition, the glacier has 3 – 60 cm thick englacial debris bands that crop out as 1 – 2 m tall ridges on the surface. This study presents the results of borehole video surveys across the transition from sliding to a frozen bed, with the goal of determining debris concentration and distribution within the terminus of the glacier. Debris content increases with distance downglacier and depth in borehole, but debris comprises only ~0.03 - 0.15% by volume relatively far downglacier, a region with comparatively high amounts of entrained debris. No large debris bands were observed in borehole video, suggesting the features that crop out on the surface are confined downglacier, having already passed the BTT. I propose two mechanisms for how basal debris can be entrained and elevated within Storglaciären: folding and thrusting of an accreted horizontal sheet of debris or injection of debris into a nonhorizontal fracture or void. With the present data, I cannot definitively distinguish between the models, but the lack of multiple generations of debris bands within Storglaciären suggests that the process responsible is infrequent, if not unique to observed bands.

Keywords: Storglaciären, debris, glacial transport, video methods, boreholes, Norrbotten Sweden

INTRODUCTION

Glaciers have the ability to erode, entrain, and transport substantial quantities of material ranging in size from clay and silt to boulders the size of houses. Glacial termini with supraglacial debris are widespread, commonly with englacial bands of debris that crop out at the surface. Debris bands have been studied on many glaciers including Kvíárjökull, Iceland (Swift et al., 2006), Haut Glacier d'Arolla, Switzerland (Goodsell et al., 2005), Matanuska Glacier, Alaska (Ensminger et al., 1999; Evenson et al., 1999; Ensminger et al., 2001), and numerous glaciers on Svalbard (Boulton, 1970; Murray et al., 1997; Hambrey et al., 1999; Hubbard et al., 2004). Bands of debris, however, are not uniform in thickness, clast grain size, or distribution across glaciers or even across a single glacier. Debris bands range in thickness from mm (Ensminger et al., 1999; Ensminger et al., 2001) to >m (Roberts et al., 2002; Swift et al., 2006) and have several possible origins, including incorporation and folding of rockfall material (Hambrey et al., 1999), basal material elevated along longitudinal folds and thrust faults (Hambrey et al., 1999; Jansson et al., 2000; Glasser et al., 2003; Hubbard et al., 2004), and injection of debris carried by high-pressure water into englacial fractures (Ensminger et al., 2001; Roberts et al., 2002).

Different methods have been applied to determine how the sediment of debris bands is initially entrained and then elevated to the surface of the glacier. For example, sedimentological studies have examined the nature of the clasts within the debris band to determine the source of the debris (Alley et al., 1997; Hambrey et al., 1999; Swift et al., 2006). Isotope data are used to constrain the age and origin of interstitial ice in debris bands (Ensminger et al., 1999; Ensminger et al., 2001; Roberts et al., 2002; Swift et al.,

2006). Researchers have also examined englacial and supraglacial structural features to examine the relationship between ice flow dynamics and debris bands (Alley et al., 1997; Murray et al., 1997; Hambrey et al., 1999; Goodsell et al., 2005; Swift et al., 2006).

In this study, I used boreholes to investigate the terminus of Storglaciären, Sweden (Fig. 1), one of the longest-studied glaciers in the world. Since 1994, debris bands have cropped out on the terminus of Storglaciären, forming prominent ice-cored ridges. The use of borehole video allows examination of the spatial distribution of debris within the terminus. I constrain the extent of the debris bands in the subsurface in order to describe how the debris was initially entrained and how the debris came to reach the surface as discrete debris bands.

BASIC GLACIOLOGY

Valley glaciers are generally confined to discrete valleys between mountains, as opposed to ice caps, which bury all topography in ice. Snow is added to valley glaciers and is then buried progressively deeper by later years' accumulation. The resulting pressure from the snow overburden gradually metamorphoses snow into subspherical crystals, known as firn, which gradually become ice over a period of years (Hooke, 2005). The resulting ice deforms due to slope and overburden pressure and flows downhill (Hooke, 2005) into the ablation zone (Fig. 2), where there is net loss of ice (van der Veen, 1999).

The temperature of the ice and the temperature at the bed are not uniform for all glaciers. Temperate glaciers, generally found at lower latitudes, contain ice at ~0°C (Hooke, 2005), where liquid water and ice are in thermal equilibrium (temperate ice). However, polar glaciers, found at higher latitudes, are colder than 0°C due to a local

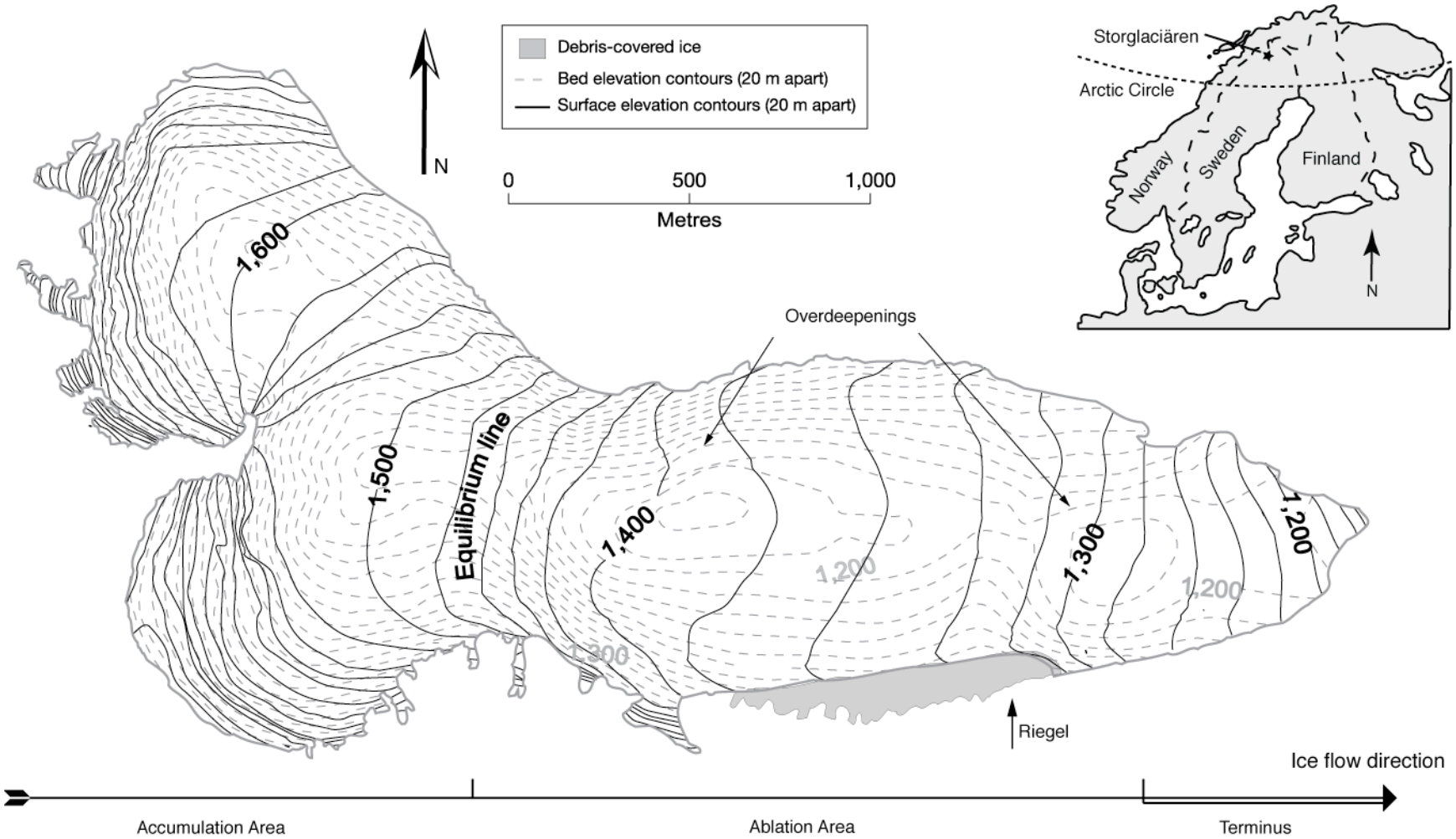

Figure 1. Location map of Storglaciären and outline of glacier. On outline, solid lines represent surface topography and dashed lines show bed topography. The two overdeepenings and the riegel in the ablation zone are labeled. Modified from Glasser et al. (2003) and Etienne et al. (2003).

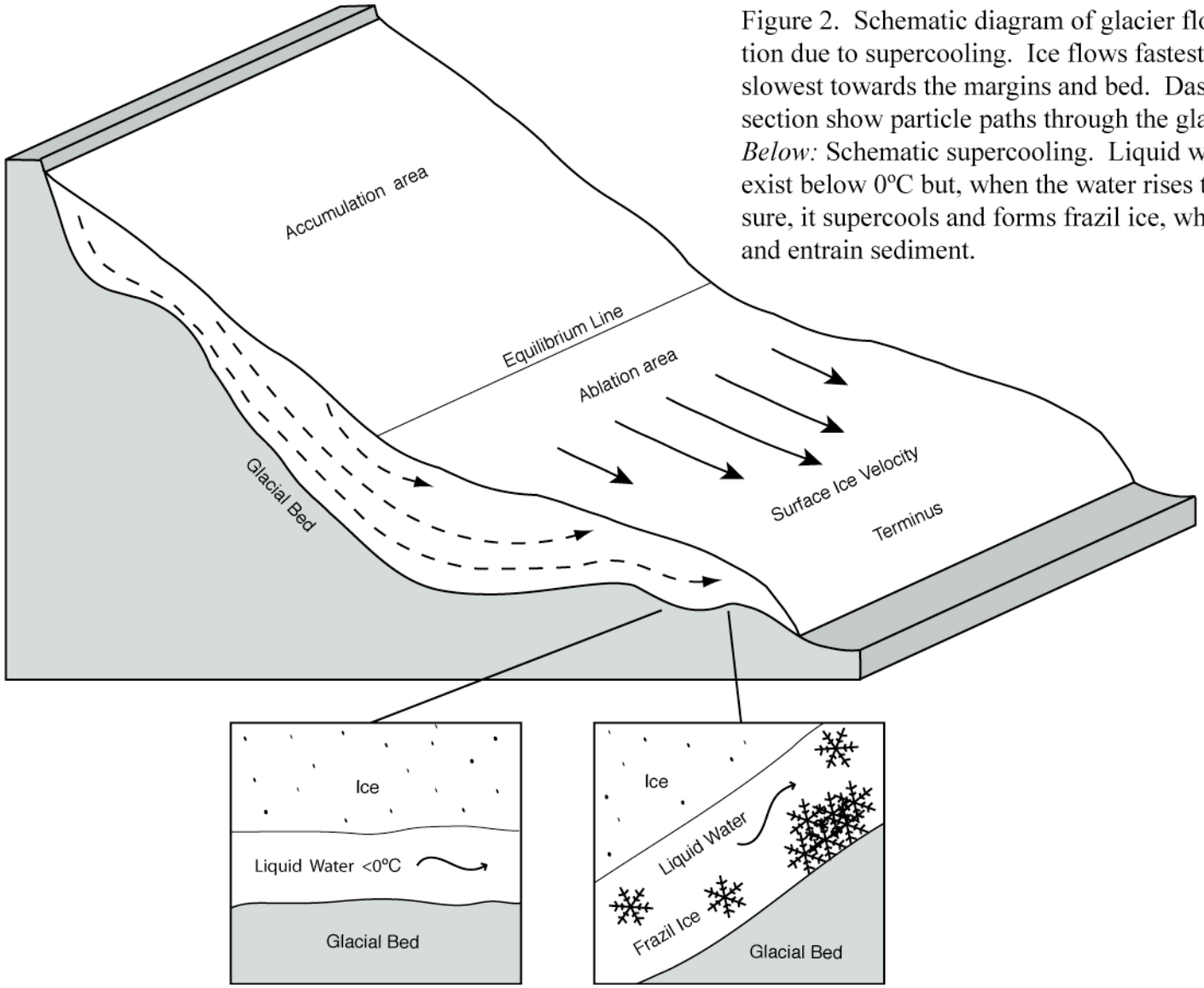

Figure 2. Schematic diagram of glacier flow and frazil ice formation due to supercooling. Ice flows fastest near the centerline, slowest towards the margins and bed. Dashed lines in cross-section show particle paths through the glacier.
Below: Schematic supercooling. Liquid water under pressure can exist below 0°C but, when the water rises to areas of lower pressure, it supercools and forms frazil ice, which can clog channels and entrain sediment.

climate with mean annual temperatures well below 0°C (Hooke, 2005).

Several factors contribute to the thermal regime of glaciers and how glaciers flow. At atmospheric pressure, the pressure melting point of ice is 0°C, but under higher pressures, the melting point decreases, allowing liquid water to exist in thermal equilibrium with ice at temperatures somewhat below 0°C (Hooke, 2005). This allows ice to exist at the pressure melting point and below 0°C and still be temperate ice. Geothermal flux can also contribute heat to a glacier, raising the temperature if the ice is <0°C (Hooke, 2005). In a temperate glacier, the combination of warmer atmospheric temperatures, depression of the pressure melting point, and the influence of geothermal flux allows liquid water to exist between grain boundaries and between the glacier and the bed. This liquid water at the base enables the glacier to slide over the bed, adding to the ice velocity due to ice deformation (Hooke, 2005). Polar glaciers however contain ice at temperatures below the pressure melting point. Polar glaciers contain little liquid water and therefore do not slide along the bed on a thin sheet of water. Ice deformation within the glacier, therefore, contributes to most of the ice velocity in these glaciers, because they are frozen to the bed (Hooke, 2005).

Polythermal valley glaciers have temperate and polar portions within a single glacier. In the ablation zone, the inner core of the glacier is at the pressure melting point (temperate ice), while the surface layer of ice (cold ice) is below the pressure melting point (Holmlund and Eriksson, 1989; Jansson, 1996). The two layers meet at the cold-temperate surface (CTS), where the temperature of the ice reaches the pressure melting point (Fig. 3). The transition from temperate ice to cold ice is visible in ground-penetrating radar images because temperate ice contains water droplets that scatter the

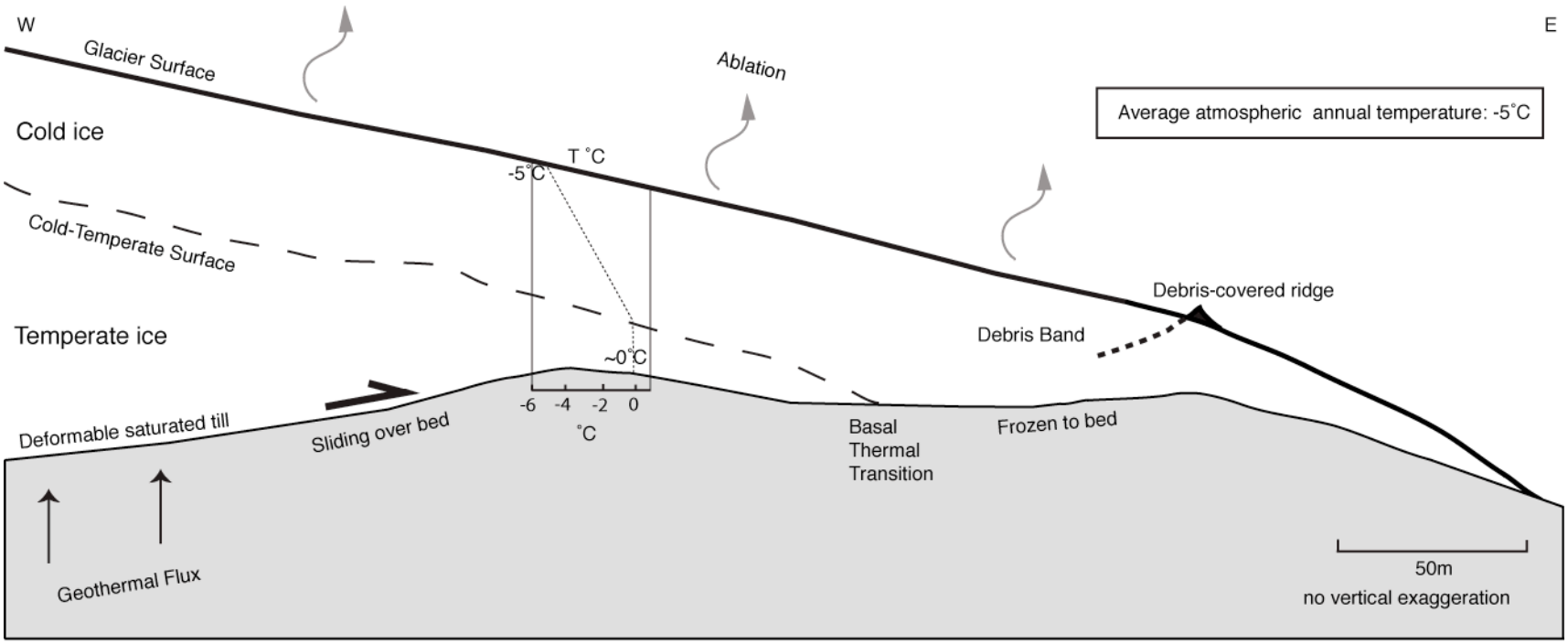

Figure 3. Cross-section of the terminus of Storglaciären, illustrating cold ice, temperate ice, and the basal thermal transition between sliding ice and ice frozen to the bed. Temperate ice slides over the bed, composed of deformable till. Cold ice is frozen to the bed at the terminus. Schematic temperature profile shows vertical temperature gradient. Debris-covered ridges shown on terminus, with inferred englacial debris band.

radar signal and the overlying cold ice is relatively transparent (Jansson et al., 2000; Glasser et al., 2003).

Depressions in the topography of the bed, overdeepenings, can have effects on the hydrology of a glacier. Liquid water at the bed is often below 0°C (Alley et al., 1999; Hooke, 2005). If the adverse (downglacier) slope of the overdeepening is steep enough, water forced up this slope cannot maintain thermal equilibrium with the changing pressure melting point (Alley et al., 1999). The liquid water supercools and can form frazil ice (Fig. 2), a distinctive morphology of ice crystals that forms in supercooled water (Evenson et al., 1999). The formation of ice releases heat enabling the remaining liquid water to stay in thermal equilibrium with the glacial ice. Frazil ice and glaciohydraulic supercooling have been proposed as means of adding ice mass to the base of a glacier as well as means of entraining debris (Alley et al., 1999; Evenson et al., 1999). Frazil ice can trap sediment suspended in a subglacial stream as it travels up the adverse slope of an overdeepening (Evenson et al., 1999).

STORGLACIÄREN

Storglaciären is a small valley glacier on the Kebnekaise massif, northern Sweden (Fig. 1). The glacier is approximately 3.2 km long and 1 km wide (Fig. 1) with a surface area of ~3 km^2 (Jansson, 1996). Storglaciären is one of six polythermal glaciers in the Kebnekaise region (Massih, 2001). The glacier has retreated over 500 m throughout the 20th century from the Little Ice Age maximum (~1910) to the current position of the terminus (Holmlund, 1987). Retreat has ceased within the last decade in part due to positive mass balance (Jansson et al., 2000).

Because Storglaciären is polythermal, and the bulk of the glacier is temperate, it slides over the bed on a thin sheet of water or saturated, easily deformable till (Jansson, 1996). This till is about 0.4 – 0.7 m thick near the middle of the ablation area based on a study conducted by Brand et al. (1988). Sliding accounts for 60 - 90% of the velocity of the surface at the glacier (Iverson et al., 1995; Jansson, 1996). Near the terminus, however, the cold ice layer is ~22 – 30 m thick (Jansson et al., 2000) and intersects the bed near the terminus (Fig. 3). This intersection marks the transition from temperate ice sliding over the bed to cold ice frozen to the bed (Glasser et al., 2003) and is referred to as the basal thermal transition (BTT).

The bedopography beneath Storglaciären (Fig. 1) contains four overdeepenings (Björnsson, 1981). The largest overdeepening occurs in the upper ablation area, closed on the downglacier end by a ridge of resistant rock, known as a riegel (Jansson, 1996). Downglacier from this riegel is another smaller overdeepening. One or both of these overdeepenings may affect the hydrology at the terminus.

The subglacial hydrologic system is highly variable. Jansson (1996) demonstrates that summer diurnal water pressure fluctuations can swing from water pressure lows near atmospheric pressure to highs at or above ice overburden pressure. Holmlund and Hooke (1983) observed multiple summertime high water pressure events near the middle of the ablation area that resulted in dramatically elevated water levels in moulins and audible cracking. Jansson (1996) also notes that several boreholes near the most downglacier overdeepening overflowed with silty water for several days in the summer of 1992. Frazil ice developed on the borehole walls, consistent with pressurized water originating at the bed (Jansson, 1996).

DEBRIS BANDS

Beginning in 1994 (Glasser et al., 2003), ice-cored debris-covered ridges have developed on the surface of the northern half of the terminus of Storglaciären (Fig. 4). These 1 – 2 m tall, arcuate ridges (Fig. 4) originate from discrete 2 – 60 cm thick regions with debris concentrations of ~50% by volume (Jansson et al., 2000) melting out and shading the ice (Jansson et al., 2000). At the surface, these debris bands dip between 50° and 70° upglacier (Glasser et al., 2003).

The debris appears to be glaciofluvial and subglacially sourced. Characteristics of the debris are consistent with subglacial till (Glasser et al., 2003). Ground-penetrating radar traces an englacial reflection (inferred to be debris) from the debris-covered ridges towards the bed (Jansson et al., 2000; Glasser et al., 2003). Uno et al. (2006) shows that interstitial ice in debris bands is significantly different than ice above and below the bands based on stable isotope and tritium studies (although less extensive studies have found no statistical difference (e.g. Glasser et al., 2003)).

BOREHOLES IN ICE

Borehole data were collected across two transects (Fig. 5) near the terminus, with twenty-four boreholes drilled using a hot water drill, consisting of a generator, a pump, a boiler, a long section of hose, and a ~1.5 m metal nozzle (cf. Hubbard and Glasser, 2005). The nozzle focused a stream of pressurized hot water downward that created a smooth-sided, nearly uniform, ~10 cm diameter borehole (Fig. 6) from the surface of the glacier to the bed. Borehole lengths ranged from ~14.3 - 42.5 m. Most boreholes were examined with a small submersible camera (cf. Pohjola, 1994; Harper and Humphrey, 1995; Fountain et al., 2005), equipped with a small wide-angle lens ringed by

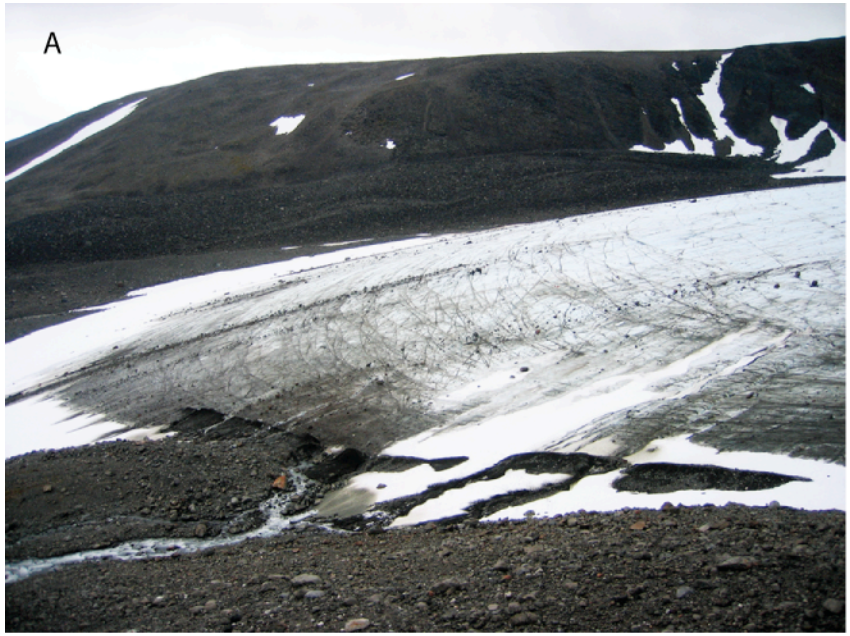

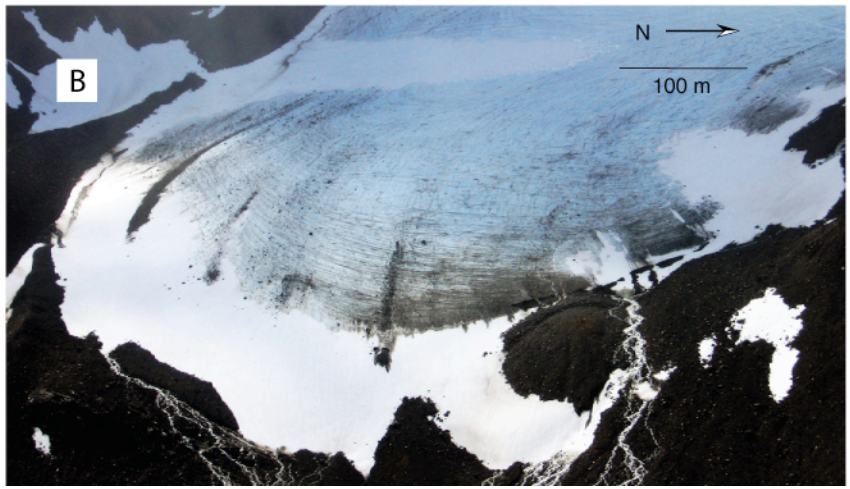

Figure 4. *A and B:* Two views of the terminus of Storglaciären. The arcuate debris-covered ridges are prominent 1 - 2 m tall features on the northern half. Rockfall debris from the accumulation zone comprise the longitudinal stripes in both views.

C: Debris-covered ice ridge bisected by supraglacial stream. Debris band is ~60 cm thick and locally contains silt to cobble-sized clasts. Large angular boulders to left are rockfall debris originating far upglacier. Ice flow is left to right, field book for scale.

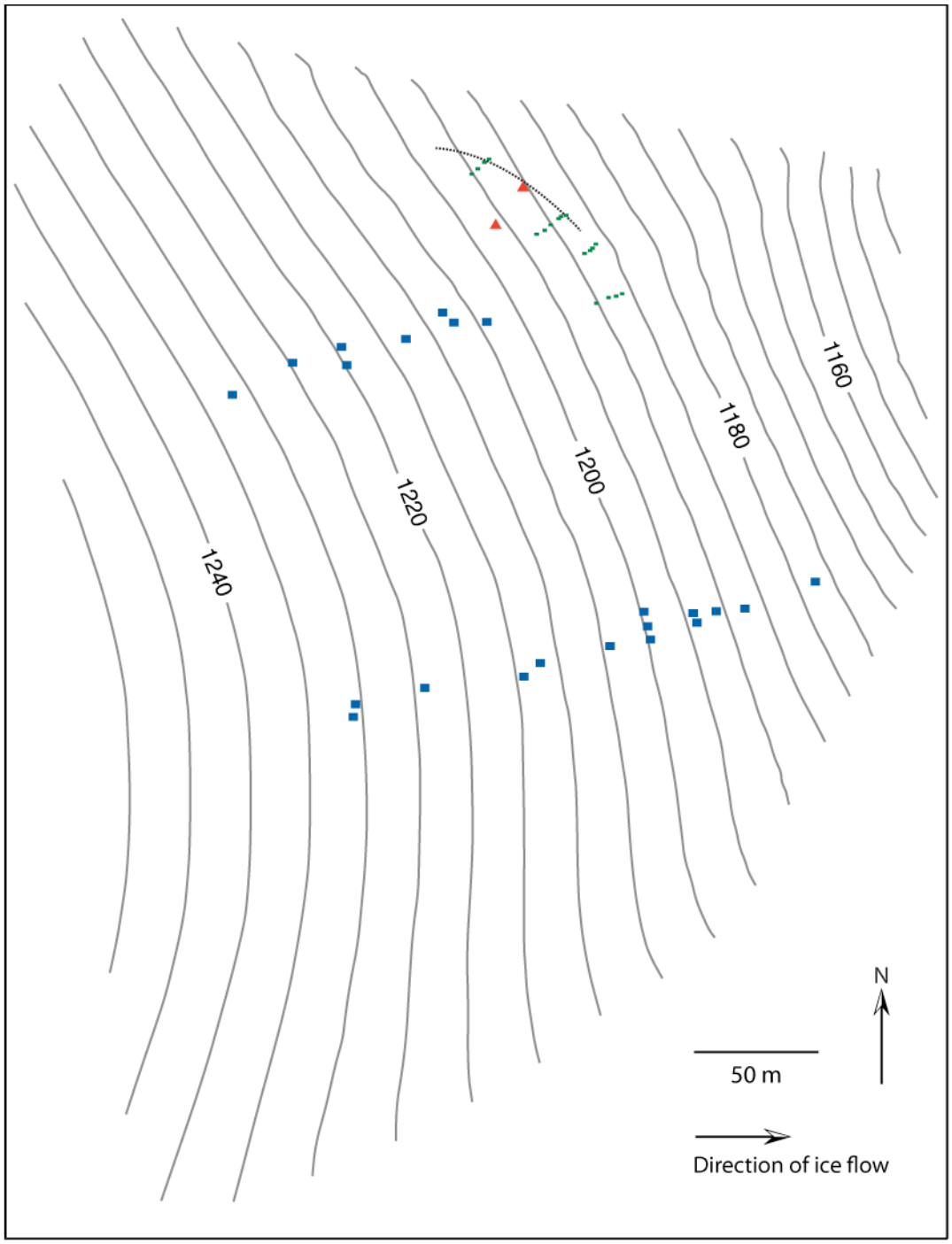

Figure 5. Topographic map of the terminus of Storglaciären showing locations of south transect and north transect (large blue dots) and Heucke drill boreholes (small green dots). The red triangles represent two springs observed on the terminus and the black dashed line is the approximate location of the debris-covered ridges.

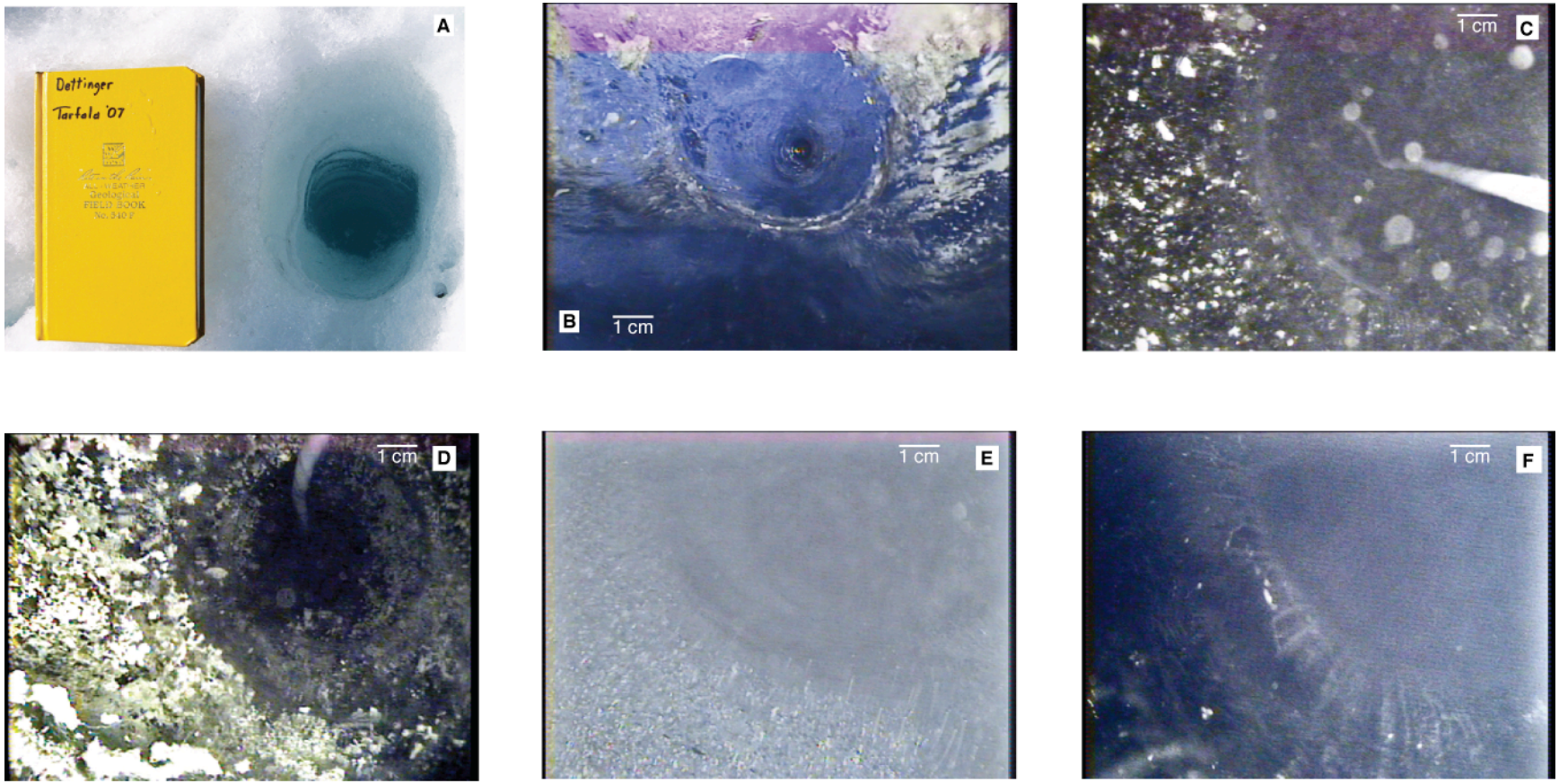

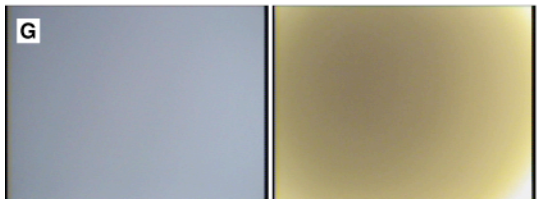

Figure 6. Borehole images. (A) Surface of boreholes with fieldbook for scale (B) dipping plane of fine grained debris in clear ice, (C) clear ice with scattered debris, ~0.5 cm diameter thermistor cable, (D) debris-rich ice, ~0.5 cm diameter thermistor cable, (E) bubbly ice, (F) clear ice, (G) typical light grey cloudiness and unusual yellow-orange cloudiness observed in four boreholes.

LEDs to shed light at depth. The camera hung from a long data cable, which was connected to a Canon GL2 camcorder. Some boreholes were filmed in their entirety, in others only distinct features were imaged, and some were too opaque to make data collection worthwhile.

Using a Heucke Steam Drill, eighteen smaller boreholes ~4 - 5 cm in diameter and between 0.5 - 8.8 m in depth were drilled in four transects across the debris-covered ridges (Fig. 5). The Heucke Drill is similar to the larger hot water drill but much smaller, more mobile, and could not penetrate regions of ice with high concentrations of debris.

BOREHOLE VIDEO ANALYSIS

The most distinct features in the borehole video are the fine layers of englacial debris. Most debris occurs as dipping mm to cm scale discrete planes of fine sediment (Fig. 6B). Debris planes are commonly observed encased in clear ice, in otherwise more bubble-rich regions. Englacial debris also occurs as disseminated specks of fine particles, with little or no overall structure (Fig. 6C), although some regions contained higher concentrations of scattered debris than others. The abundance of debris planes and disseminated debris increases with depth and distance downglacier (Fig. 6D) and both forms of debris are nearly absent from the entire sections of the most upglacier boreholes.

Bubbles, <mm diameter, in glacial ice were observed in all boreholes. Bubbles are particularly distinct because they reflect the light of the camera unlike clear ice (Figs. 6E and 6F). Bubbles, like englacial debris, can also form planar features, often dipping parallel or subparallel to nearby debris planes. In contrast to the trend of debris concentration, bubble content in the glacial ice decreases with depth and distance downglacier. The near-surface portions of most borehole walls are nearly opaque with

bubbles, although at the extremely near-surface (within ~50 cm), water-filled grain boundaries are likely to reflect light as well (Moore, 2008, personal commun.). Regions with high bubble content can also alternate with regions devoid of bubbles.

Despite the abundance of fine planes of englacial debris, the 2 – 60 cm thick debris bands that crop out at the surface were not visible in the video of boreholes farther upglacier. Boreholes in the lower portion of the north transect contained relatively high concentrations of debris in abundant dipping planes (Fig. 6D), but nothing as discrete or thick as those that crop out at the surface. However, in the same transect, in the process of drilling the borehole farthest downglacier, a region that felt like dense debris was encountered at ~10 m. Drilling slowed dramatically, but unlike hitting the solid bed, the drill continued to make progress. A knocking feeling was also reported, interpreted as debris agitated by the jet of water and hitting the nozzle. Borehole video, however, only revealed a strange undulating cloud of silt-laden water at 9.5 m, below which suspended silt made the water too opaque to see the borehole walls.

Also notably absent from the borehole video were englacial voids, fractures, and conduits. In a total of 23 boreholes, only one englacial opening was observed directly in borehole video. The lone fracture occurs near the middle of the ice thickness partway down the south transect. In contrast, a concentration of ~2 voids per borehole has been reported in the middle of the ablation zone (Fountain et al., 2005).

The murkiness of the water universally increased with depth in boreholes. Most boreholes became too opaque to even make out the walls less than a centimeter away. In a number of boreholes in the north transect, the murkiness significantly changed color at a certain depth. This pronounced color change from the typical blue-grey color to an

orange-yellow hue (Fig. 6G) occurred between 4 – 6 m above the bed in four of the seven boreholes examined in the north transect. Similar murk color changes are absent in videos of the south transect.

The suspended sediment in some boreholes had the chance to settle out, collecting at the bottom of the borehole. Estimates were obtained of debris concentrations in the downglacier portion of the north transect by comparing the apparent bottom of the borehole visible in the video to the length of thermistor cable buried in the sediment at the base of the hole. The lengths of thermistor cable buried in the accumulated sediment correlate closely with the reported depths to which the boreholes were drilled. Two boreholes ~10 m apart yielded concentrations of 0.03 and 0.13 m^3 of debris per cubic meter of glacial ice, respectively. A borehole, possessing an apparent depth that differed from original drilling depth but without a thermistor cable to corroborate, in the south transect yielded an estimate of 0.15 m^3 of debris per cubic meter of glacial ice.

MAPPING DEBRIS BANDS

Because the smaller Heucke steam drill cannot penetrate extremely debris-rich regions, the length of the boreholes was used as a proxy for the debris bands. Heucke borehole depths shallow with increasing proximity to the debris-covered ridges (Fig. 7). Downglacier from the ridge, no limit was observed on how deep a borehole could be drilled, suggesting a dramatic change in debris concentrations between upglacier and downglacier of the ridges. This pattern held true even in the two transects closer to the glacier centerline where no outcrops of thick debris bands occur.

Surface dips taken on the debris band ranged from 60° and 70° near the northwestern end of the debris-covered ridges to 31° and 45° near the southeastern

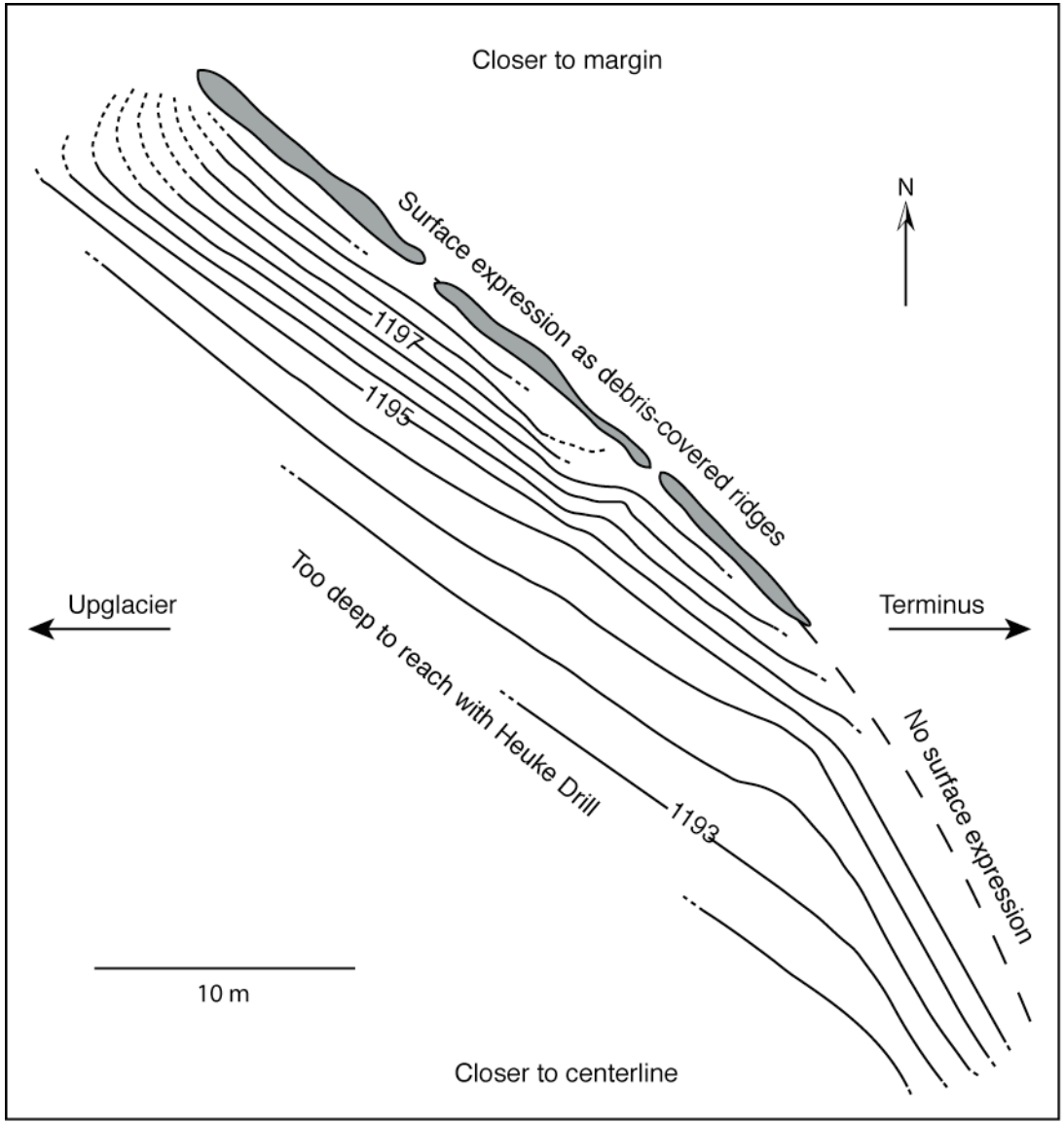

Figure 7. Structure contour map of debris band in the subsurface based on penetration depths of Heucke boreholes. Upglacier dip is shallow in the SE (~25.8°) and steepens to the NW (39.4°). Ice flow is from left to right. The small dashes represent limits of where Surfer could extrapolate using available data. The intersection with glacier surface marked with debris ridges or large dashes. Contour interval is 0.5 m.

portion, closer to the glacier centerline, suggesting changing dips along the length of the debris band. A structure contour map of the debris band generated by Golden Software's Surfer, using the borehole depths as a proxy for the surface of debris-rich regions, produces estimated dips of ~40° in the northwest and ~26° in the southeastern portion of the feature (Fig. 7). The debris band therefore appears to change dip along strike, shallowing with proximity to the glacier centerline, and steepening with proximity to the surface.

MODELS FOR DEBRIS BAND FORMATION

Most researchers agree that the debris that is now cropping out on the surface of Storglaciären originated at the bed as a part of the 0.4 – 0.7 m thick till layer (Jansson et al., 2000; Glasser et al., 2003). However, there are two models that explain how the thick, discrete debris bands were initially entrained and how they reached the surface. The first model, typically used to explain the debris bands on Storglaciären, involves accretion of ice and sediment to the base of the glacier at the BTT and subsequent folding and/or thrusting due to the change from basal sliding to a frozen bed at the BTT (Jansson et al., 2000; Glasser et al., 2003). The second model involves pressurized subglacial water and injection of debris into an opening within the glacier and is subsequently rotated by differential ice velocity. Both models are discussed in more detail below.

Thrust fault model

The first model relies on a change in ice flow near the terminus that causes local compressive flow, creating conditions that both entrain and elevate basal debris (Fig. 8). In time1, debris must first be incorporated or accreted, such as through regelation (melting of ice under pressure in front of an obstacle and refreezing of derived melt water

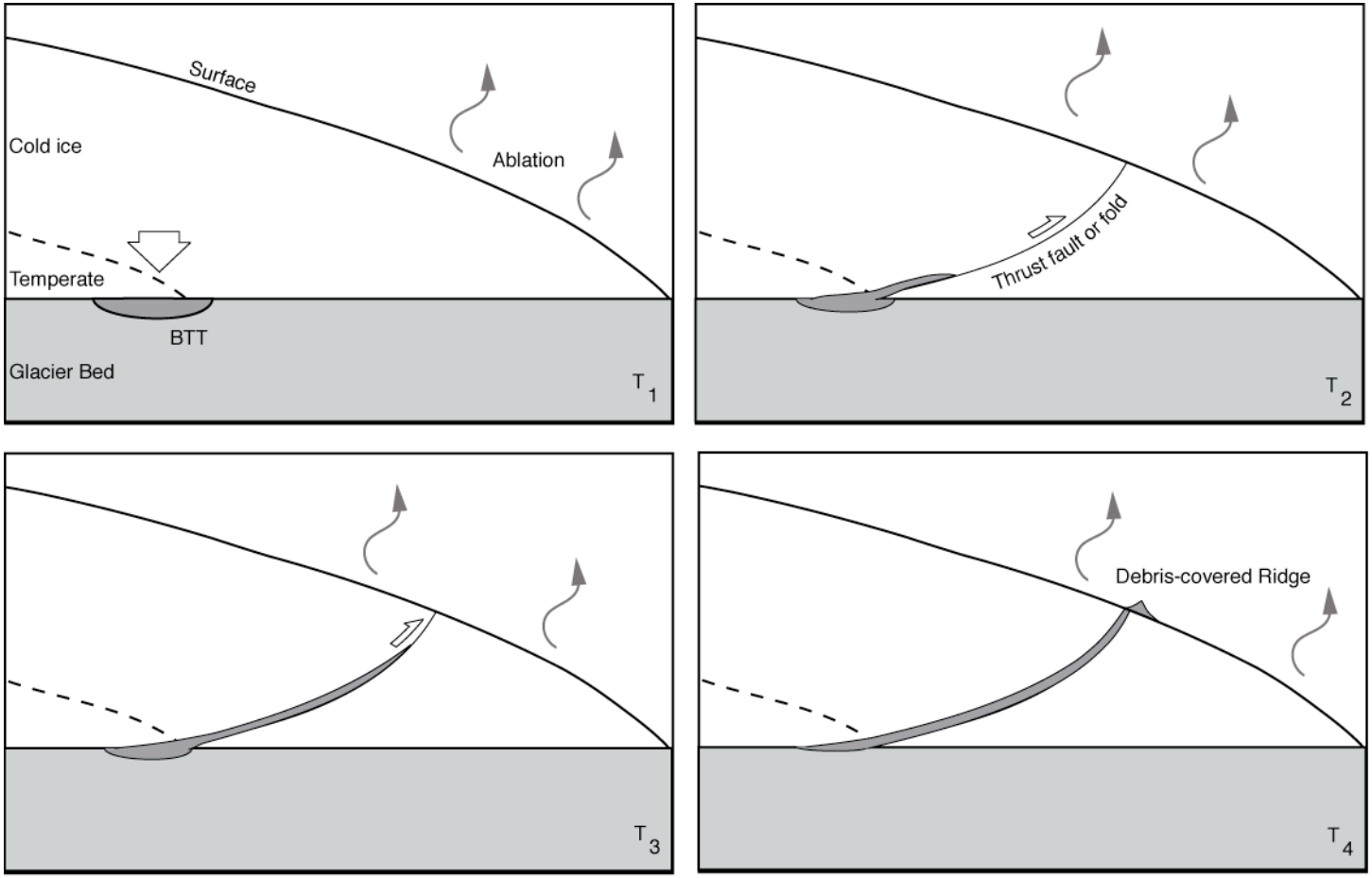

Figure 8. Schematic diagram of debris band genesis through thrusting/folding. Time1 shows regelation into basal sediments, accreting debris to the base of the glacier in the vicinity of the BTT. Time2 illustrates initiation of thrusting/folding originating at the BTT. Time3 represents continued transport of basal sediments towards the surface. Time4 represents the final position of entrained debris within the terminus and formation of debris-covered ridges when the debris band reaches the surface. Modified from Swift et al. (2006).

behind the obstacle (Hooke, 2005)) into basal sediments, before the debris can be elevated as a debris band. When stress between the faster moving sliding ice and slower nonsliding ice reaches a point high enough to fracture the ice in time2, a thrust fault forms, transporting some of the debris-rich ice along the hanging wall. As ablation continuously removes ice from the surface and with further motion along the fault in time3, the debris feature becomes closer and closer to the surface. At time4, the debris crops out on the surface and forms the debris-covered ridges observed on Storglaciären. For this model of debris band formation, dip is steepest near the surface and shallows with depth.

This model has been applied to debris bands in Iceland where Swift et al. (2006) observe >m-thick bands of poorly sorted debris with clasts ranging from silt to small boulders. Individual debris bands are tens of m apart near the centerline, closer together at the margins, and are composed of thin layers of debris-rich ice, which alternate with debris-poor ice (Swift et al., 2006). Swift et al. (2006) interpret the debris bands as basal ice and debris thickened by local compressive flow and elevated along folds and/or thrusts. Glasser et al. (2003) suggest that debris on Storglaciären was originally entrained by regelation, which incorporated sediment into the sole of the glacier, and the debris was subsequently dragged upwards along folds and thrusts at the BTT.

Debris injection model

A second model for the origin of thick bands of debris is hydraulic injection of debris into void spaces within the glacier (Fig. 9). This model relies on the presence of high fluid pressure at the base of the glacier. High water pressure (equal to or greater than the ice overburden pressure) can keep englacial fractures, such as partially

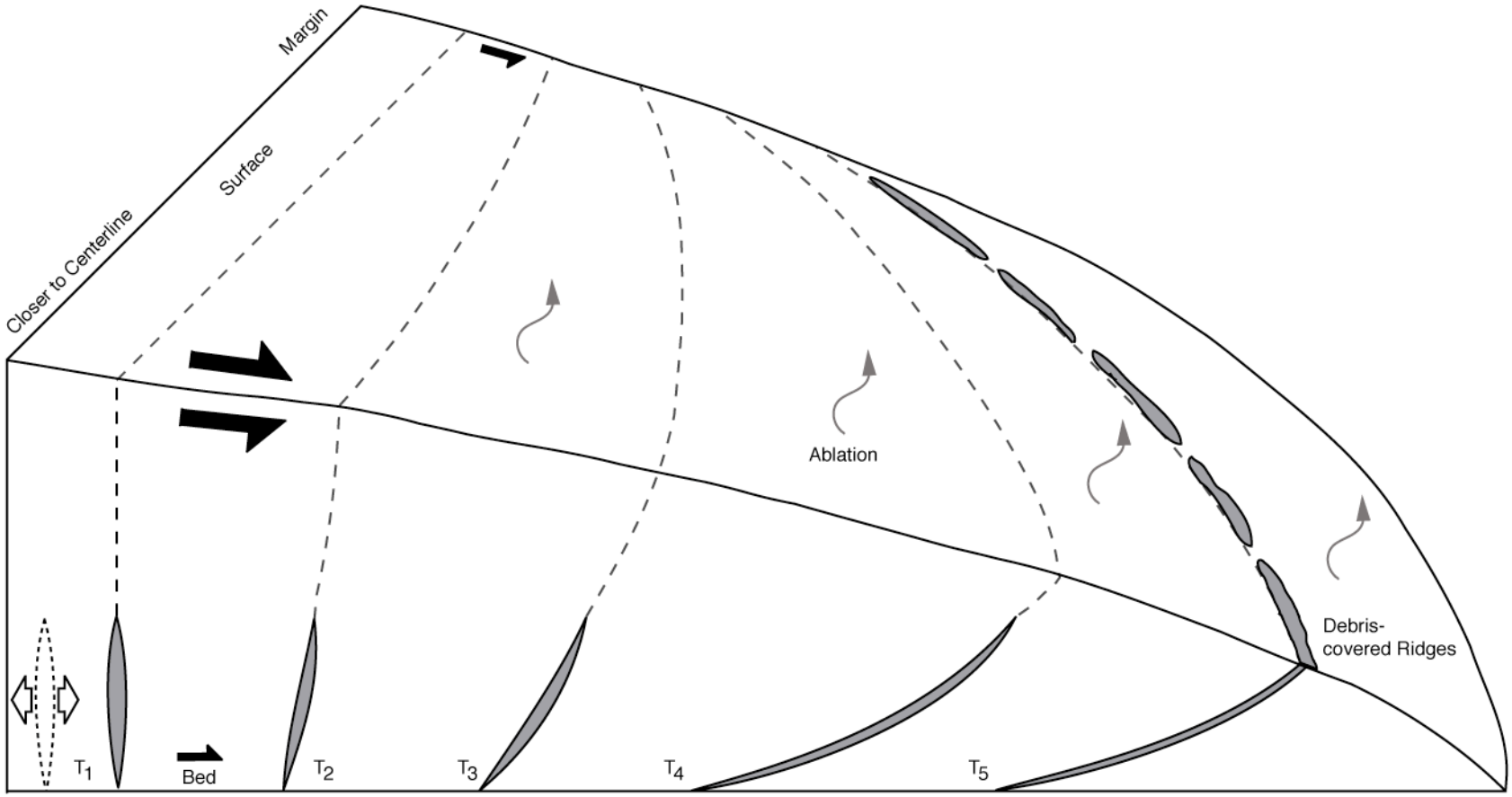

Figure 9. Schematic diagram of debris band formation through injection of debris into fractures or void space at the base of the glacier. Dark solid arrows represent different ice speeds - slower towards the margin and bed. Time1 shows opening of a fracture/void in a region of local extension (dashed cavity) and infilling of this void with sediment. The dashed line represents the initial vertical and linear orientation of the feature. Time2, time3, and time4 represent deformation of the feature both in cross-section and in map view. Time5 illustrates the creation of debris bands as ablation exposes the entrained debris. Note how the orientation of an initially vertical feature closely resembles that of horizontally accreted debris elevated along thrusts/folds (Fig. 8).

healed crevasses, from closing (Hooke, 2005) and extremely high water pressure can propagate existing weaknesses or fractures in glacial ice (Roberts et al., 2002). A void might serve as a pathway for glaciohydraulically supercooled water flow, entraining debris and injecting the debris into the fracture (c.f. Ensminger et al., 2001; Roberts et al. 2002). As illustrated in figure 9, extensional forces near the bed open a void or fracture, into which debris is emplaced at time1. The initially vertical linear feature is then subject to different ice speeds across the glacier at time2, because ice flows fastest at the surface near the centerline, slower towards the margins and the bed. Ablation continuously removes ice from the surface during time3, gradually unroofing the debris feature until the debris-rich ice is exposed at the surface, forming a debris band at time4. As with the thrust model, the injection model forms a debris band geometry where the dip is steepest near the surface and shallows with depth.

This model is used by Ensminger et al. (2001) to explain mm-scale fine-grained debris bands at the terminus of Matanuska Glacier, Alaska. The authors report audible cracking and ice-quakes on Matanuska Glacier and infer that fractures open as basal crevasses, which subsequently fill with debris, in a region of high water pressure and extension over an overdeepening. On two Icelandic glaciers Skeidararjokull and Skaftafellsjokull, Roberts et al. (2002) report “fracture fills,” ~30° upglacier dipping bands of coarse-grained sand that rangedfrom <1 cm to 5 m thick, related to a 1994 glacier-outburst flood, known as a jökulhlaup. Extremely high-pressure water cracked the ice and, as water escaped through the fractures to regions of lower pressure, frazil ice resulting from the supercooled water caused instantaneous freeze-on of sediment to the

fracture walls (Roberts et al., 2002). The "fracture fills" remain as discrete debris bands that crop out on the surface.

APPLICATION TO STORGLACIÄREN

Thrust fault model

Predicted basal water pressures needed to accrete debris through regelation differ from those observed beneath Storglaciären. Regelation into basal debris has been experimentally shown to occur when ice pressure is significantly higher than the pore water pressure in basal sediment and has implications for entraining 0.1 – 1 m thicknesses of debris (Iverson, 1993; Iverson and Semmens, 1995; Alley et al., 1997). However, the extremely low water pressures required for regelation into basal debris are unlikely to occur in overdeepenings (Swift et al. 2006) or near the terminus in the winter when basal water pressures reach and exceed the overburden pressure for extended periods of time (Moore, 2008, personal commun.).

Ice speed differences between sliding ice and nonsliding ice may result in elevated strain rates and possible fracturing of the ice, but these predicted patterns do not match preliminary strain rate data or velocity data. Glasser et al. (2003) propose that the debris is then caught up in folds and thrusts caused by glaciotectonic compression at the BTT, where sliding temperate ice meets slower frozen-to-the-bed cold ice (Fig. 8). Alley et al. (1997) note that, in general, thrusts and folds are relatively limited to the vicinity of the bed, rising no more than about 10 – 20 m, approximately the ice thickness of Storglaciären near the thick debris bands (Glasser et al., 2003). Horizontal velocity has been shown to slow ~50% across the region containing the debris bands (Jansson et al., 2000) and this is likely due to frozen bed conditions. However, the strain rates at the

BTT may not be high enough to form thrust faults or discrete shear zones in the ice. The transition from sliding to a frozen bed appears to be gradual, suggesting strain rates are low (Moore, 2008, personal commun.). Velocity data (Fig. 10) indicate there is no significant increase in emergence velocity (upward-directed rather than horizontally-directed motion) for corresponding decreases in horizontal velocity. The lack of an increase in emergence velocity, no development of a fault scarp or additional topography on the hanging wall of a fault, and the lack of multiple generations of debris bands suggest that thrusting is infrequent or not tied to the formation of the debris bands.

The thrust fault model conforms well to timing data. Jansson et al. (2000) conservatively predict that transportation through the ice along a thrust fault or fold took ~14 years due to local ice velocity and distance of debris-covered ridges from the BTT. Fourteen years is well within the time constraint suggested by tritium (^{3}H) data because the debris band ice (~4 TU) has been shown by Uno et al. (2006) to be post-1952 atmospheric nuclear testing, while ice above and below the debris bands (~0 TU) appears to be pre-1952 (Singh and Kumar, 2005).

Debris injection model

Storglaciären has not experienced any events as dramatic as a jökulhlaup in over sixty years of continuous monitoring, but the variable water pressure within and beneath the glacier appears to be high enough to occasionally fracture weaknesses in the ice. Holmlund and Hooke (1983) report audible cracking and ice-quake activity, associated with water pressures equal to or greater than the ice overburden pressure in an overdeepening and which might result in the formation of fractures near the sole of the

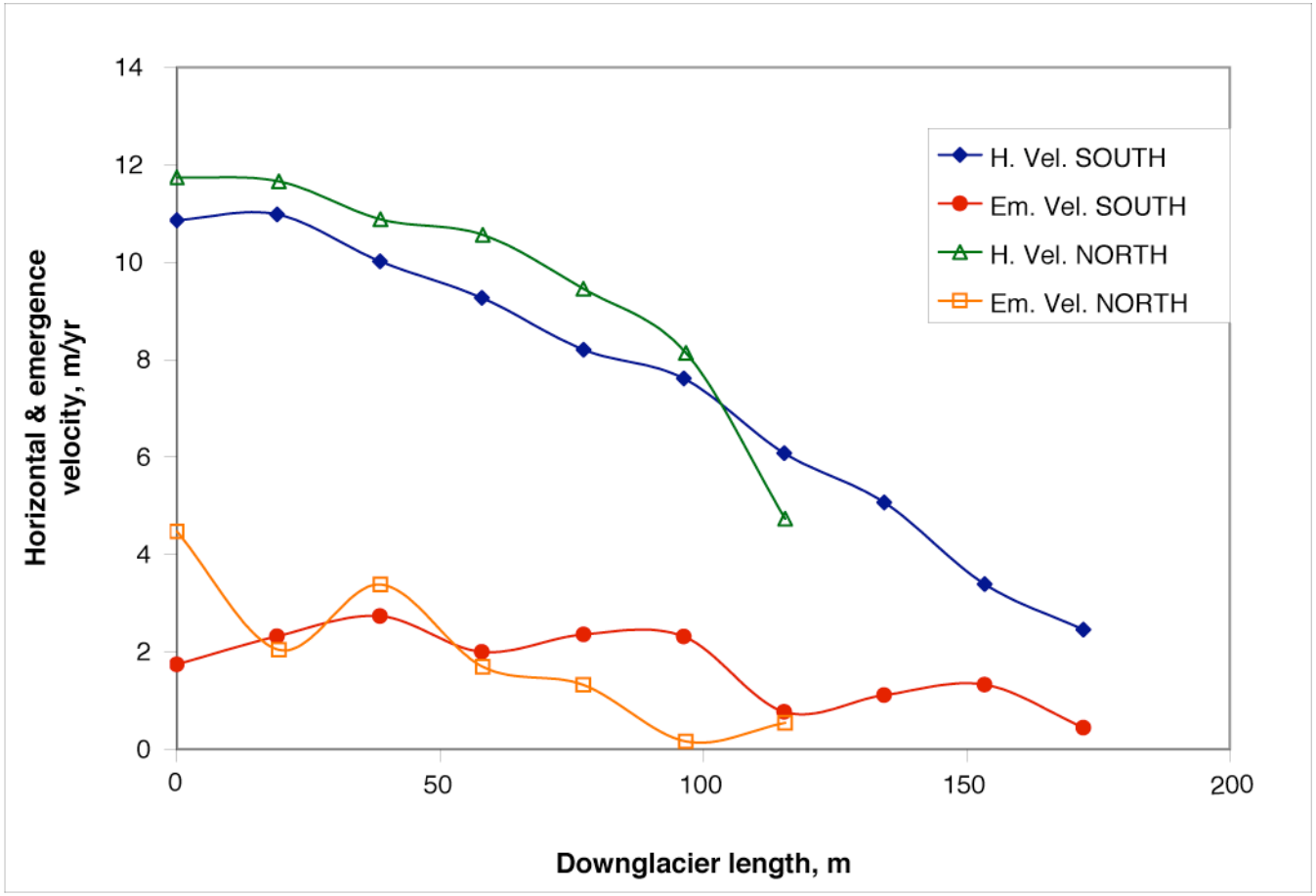

Figure 10. Velocity data from the terminus. The diamonds and triangles show horizontal ice velocity and the circles and squares show emergent ice velocity for the two transects. Note that there is no significant increase in emergent velocity in response to decreasing horizontal velocities. Modified from Moore (2008, personal commun.).

glacier. But in the absence of dramatic events such as jökulhlaups, the creation of 60 cm wide, ~70 m long fractures seems unlikely to occur. However, the possibility of a crevasse from the upglacier crevasse field remaining only partially healed and serving as required void space is feasible (Moore, 2007, personal commun.). The similarity of reported ice-quake activity to that reported on Matanuska Glacier, periods of sustained high water pressure, an overdeepening, and direct observation of supercooled water on Storglaciären suggests that the conditions to form basal fractures filled with debris are satisfied.

In the injection model, the debris may have been emplaced through fluid transport, but observed clast size distribution differs from predictions. Supercooled water is unlikely to be responsible for the unsorted sand and cobble-sized clasts observed within the bands due to the sorting of sediment expected with current. Also, extremely high flow velocities would be needed to entrain such large clasts in a vertical void.

Assuming fluid-carried debris injection, the importance of liquid water and unfrozen basal debris constrains the location of emplacement to upglacier of the BTT. The <56 year age of the debris bands constrains the upper limit of where the debris bands could have formed to the crevasse field over the riegel of the large overdeepening (Fig. 1). Ice at the crevasse field takes >50 years to reach the current position of the debris bands at present ice speeds (Moore, 2008, personal commun.). Interstitial ice freezing upglacier of the crevasse field would have had to form too long ago to record elevated post-1952 tritium levels.

Summary

In comparison, the expected end result of one model looks very much like that of

the other model. The BTT likely affects flow dynamics at the terminus, but the degree to which thrusting and/or folding originates at this transition is unclear. Certain features that might occur on an actively thrusting/folding glacier terminus are absent on Storglaciären. The alternative injection model relies on elevated water pressures, observed on Storglaciären, but cannot account for the size of large entrained clasts.

CONCLUSIONS

Borehole video of Storglaciären constrains debris concentrations and distribution within the terminus of the glacier. Within boreholes, I generally observed small amounts of debris, which increased in concentration with depth and distance downglacier, comprising ~0.03 - 0.15% of the glacier nearest the terminus. The debris forms thin dipping planes or disseminated specks within the ice but no thick cm – dm scale debris bands like those that crop out on the terminus were observed. Therefore, the thick debris bands appear to be constrained to a limited englacial area at the very terminus.

Two mechanisms for the formation of the debris bands have been proposed: (1) accretion of a horizontal sheet at the BTT, which was then brought to the surface along thrust faults or longitudinal folds, or (2) the injection of debris into a nonhorizontal fracture and subsequent differential ice flow deformation and ablation exposing the band at the surface. With the present data set, I cannot determine which model is most appropriate. However, the lack of multiple generations of debris bands suggests that the process that entrained and elevated the debris is infrequent, if not unique to the present debris bands.

ACKNOWLEDGEMENTS

I would like to thank my advisors: Pete Moore (Iowa State University) for the opportunity to spend an amazing field season in the Swedish Arctic and his tireless efforts helping me with the research and answering silly questions, and Sarah Titus (Carleton College) for helping me when I struggled with prose, figures, or mind-hurting math. Thanks also to the rest of Team America for great times at Tarfala, the geology majors (especially Kristen Sweeney, a.k.a. Ducky or Weenz, for baked goods and pancakes) and to all of the geo seniors, especially the Muddwellers, for their incredible camaraderie and help.

Funding for this project was provided through Carleton College's Class of 1963 Fellowship.

REFERENCES CITED

Alley, R. B., Cuffey, K. M., Evenson, E. B., Strasser, J. C., Lawson, D. E., and Larson, G. J., 1997, How glaciers entrain and transport basal sediment; physical constraints: Quaternary Science Reviews, v. 16, no. 9, p. 1017-1038.

Alley, R. B., Strasser, J. C., Lawson, D. E., Evenson, E. B., and Larson, G. J., 1999, Glaciological and geological implications of basal-ice accretion in overdeepenings, *in* Mickelson, D. M., and Attig, J. W., eds., Glacial Processes Past and Present: Boulder, Colorado, USA, Geological Society of America, p. 1 - 9.

Björnsson, H., 1981, Radio-echo sounding maps of Storglaciären, Isfallsglaciären, and Rabots Glaciär, northern Sweden: Geografiska Annaler, v. 63A, p. 225-231.

Boulton, G. S., 1970, On the origin and transport of englacial debris in Svalbard glaciers: Journal of Glaciology, v. 9, no. 56, p. 213-229.

Brand, G., Pohjola, V., and Hooke, R. L., 1988, Evidence for a till layer beneath Storglaciaeren, Sweden, based on electrical resistivity measurements: Journal of Glaciology, v. 33, no. 115, p. 311-314.

Ensminger, S. L., Alley, R. B., Evenson, E. B., Lawson, D. E., and Larson, G. J., 2001, Basal-crevasse-fill origin of laminated debris bands at Matanuska Glacier, Alaska, U.S.A: Journal of Glaciology, v. 47, no. 158, p. 412-422.

Ensminger, S. L., Evenson, E. B., Larson, G. J., Lawson, D. E., Alley, R. B., Strasser, J. C., Kleman, J., Holmlund, P., and Jansson, P., 1999, Preliminary study of laminated, silt-rich debris bands; Matanuska Glacier, Alaska, U.S.A, Annals of Glaciology, vol.28, p. 261-266.

Etienne, J. L., Glasser, N. F., and Hambrey, M. J., 2003, Proglacial sediment-landform associations of a polythermal glacier: Storglaciaren, northern Sweden: Geografiska Annaler Series a-Physical Geography, v. 85A, no. 2, p. 149-164.

Evenson, E. B., Lawson, D. E., Strasser, J. C., Larson, G. J., Alley, R. B., Ensminger, S. L., and Stevenson, W. E., 1999, Field evidence for the recognition of glaciohydrologic supercooling, *in* Mickelson, D. M., and Attig, J. W., eds., Glacial Processes Past and Present: Boulder, Colorado, USA, Geological Society of America, p. 23 - 35.

Fountain, A. G., Jacobel, R. W., Schlichting, R., and Jansson, P., 2005, Fractures as the main pathways of water flow in temperate glaciers: Nature, v. 433, no. 7026, p. 618-621.

Glasser, N. F., Hambrey, M. J., Etienne, J. L., Jansson, P., and Pettersson, R., 2003, The origin and significance of debris-charged ridges at the surface of Storglaciaren,

northern Sweden: Geografiska Annaler Series a-Physical Geography, v. 85A, no. 2, p. 127-147.

Goodsell, B., Hambrey, M. J., and Glasser, N. F., 2005, Debris transport in a temperate valley glacier; Haut Glacier d'Arolla, Valais, Switzerland: Journal of Glaciology, v. 51, no. 172, p. 139-146.

Hambrey, M. J., Bennett, M. R., Dowdeswell, J. A., Glasser, N. F., and Huddart, D., 1999, Debris entrainment and transfer in polythermal valley glaciers: Journal of Glaciology, v. 45, no. 149, p. 69-86.

Harper, J. T., and Humphrey, N. F., 1995, Borehole video analysis of a temperate glacier's englacial and subglacial structure - Implications for glacier flow models: Geology, v. 23, no. 10, p. 901-904.

Holmlund, P., 1987, Mass balance of Storglaciaeren during the 20th century, scale 1:10,000.

Holmlund, P., and Eriksson, M., 1989, The cold surface-layer on Storglaciären: Geografiska Annaler Series a-Physical Geography, v. 71, no. 3-4, p. 241-244.

Holmlund, P., and Hooke, R. L., 1983, High water-pressure events in moulins, Storglaciären, Sweden: Geografiska Annaler Series a-Physical Geography, v. 65A, no. 1-2, p. 19-25.

Hooke, R. L., 2005, Principles of glacier mechanics: New York, Cambridge University Press.

Hubbard, B., and Glasser, N., 2005, Field Techniques in Glaciology and Glacial Geomorphology: Hoboken, NJ, USA, John Wiley & Sons, LTD, 400 p.

Hubbard, B., Glasser, N., Hambrey, M., and Etienne, J., 2004, A sedimentogological and isotopic study of origin of supraglacial debris bands; Kongsfjorden, Svalbard: Journal of Glaciology, v. 50, no. 169, p. 157-170.

Iverson, N. R., 1993, Regelation of ice through debris at glacier beds; implications for sediment transport: Geology, v. 21, no. 6, p. 559-562.

Iverson, N. R., Hanson, B., Hooke, R. L., and Jansson, P., 1995, Flow mechanism of glaciers on soft beds: Science, v. 267, no. 5194, p. 80-81.

Iverson, N. R., and Semmens, D. J., 1995, Intrusion of ice into porous media by regelation; a mechanism of sediment entrainment by glaciers: Journal of Geophysical Research, v. 100, no. B6, p. 10,219-10,230.

Jansson, P., 1996, Dynamics and hydrology of a small polythermal valley glacier: Geografiska Annaler Series a-Physical Geography, v. 78A, no. 2-3, p. 171-180.

Jansson, P., Naslund, J.-O., Pettersson, R., Richardson-Naslund, C., and Holmlund, P., 2000, Debris entrainment and polythermal structure in the terminus of Storglaciaren, *in* Nakawo, M., Raymond, C. F., and Fountain, A., eds., IAHS-AISH Publication, vol.264, p. 143-151.

Massih, E., 2001, Regional variations of the cold surface layer of northern Scandinavian glaciers: Tarfala Research Station Annual Report, v. 2001-2002, p. 2 - 6.

Murray, T., Gooch, D. L., and Stuart, G. W., 1997, Structures within the surge front at Bakaninbreen, Svalbard, using ground-penetrating radar, *in* Whillans, I. M., Fountain, A., Glen, J., Jansson, P., Kohler, J., Kuhn, M., and Moore, J., eds., Annals of Glaciology, vol.24, p. 122-129.

Pohjola, V. A., 1994, TV-video observatiosn of englacial voids in Storglaciären, Sweden: Journal of Glaciology, v. 40, no. 135, p. 231-240.

Roberts, M. J., Tweed, F. S., Russell, A. J., Knudsen, O., Lawson, D. E., Larson, G. J., Evenson, E. B., and Bjornsson, H., 2002, Glaciohydraulic supercooling in Iceland: Geology, v. 30, no. 5, p. 439-442.

Singh, B. P., and Kumar, B., 2005, Isotopes in Hydrology, Hydrogeology and Water Resources, Alpha Sciences Int'l, Ltd., 188 p.

Swift, D. A., Evans, D. J. A., and Fallick, A. E., 2006, Transverse englacial debris-rich ice bands at Kviarjokull, southeast Iceland: Quaternary Science Reviews, v. 25, no. 13-14, p. 1708-1718.

Uno, K. T., Cerling, T. E., Solomon, D. K., Iverson, N. R., and Jansson, P., 2006, Stable isotope, tritium, and noble gas data from debris-rich ice on Storglaciären, Sweden, American Geophysical Union: San Francisco.

van der Veen, C. J., 1999, Fundamentals of Glacier Dynamics: Rotterdam, Netherlands, A.A. Balkema, 462 p.